

The circular jump is a white hole

G. Jannes,¹ R. Piquet,^{1,2} P. Maïssa,¹ C. Mathis,¹ and G. Rousseaux¹

¹*Université de Nice Sophia Antipolis, Laboratoire J.-A. Dieudonné,
UMR CNRS-UNS 6621, Parc Valrose, 06108 Nice Cedex 02, France*

²*Université Pierre et Marie Curie Paris VI, 4 Place Jussieu, 75005 Paris, France*

(Dated: October 11, 2010)

We provide an experimental demonstration that the circular hydraulic jump represents a hydrodynamic white hole or gravitational fountain (the time-reverse of a black hole) by measuring the angle of the Mach cone created by an object in the “supersonic” inner flow region. We emphasise the general character of this gravitational analogy by showing theoretically that the white hole horizon constitutes a stationary and spatial saddle-node bifurcation within dynamical-systems theory. Some perspectives are outlined on the usefulness of the circular jump as an experimentally viable white hole model for analogue gravity, in particular with respect to the ongoing debate on the robustness of Hawking radiation.

PACS numbers: 47.15.gm, 47.55.N-, 47.40.Ki, 04.70.-s, 04.80.Cc

A vertical fluid jet impacting on a horizontal plate forms, within a wide range of parameters, a thin layer which expands radially and is surrounded by a sudden circular hydraulic jump. The first modern description of this phenomenon dates back to Lord Rayleigh [1], who developed a momentum-balance theory to describe it, but did not take viscosity into account. The standard theory for viscous fluids is due to Watson [2], and has been further improved through the inclusion of surface tension by Bush and Aristoff [3].

The circular jump is an intricate phenomenon of fluid dynamics: while it suffices to open a kitchen tap to observe it, the theory describing it becomes tremendously complicated for all except its most simple applications. For example, the appearance of more exotic forms such as polygons [4], through variations of the surface tension [5] or when the liquid flows over micro-textured surfaces [6], has been studied experimentally but a solid understanding at the theoretical level is still in its infancy. Even for the simple circular jump in a viscous fluid with non-negligible surface tension, the standard Watson-Bush theory leads to a rather involved expression for the jump radius, which at small flow rates differs by easily 10 to 25% from the experimentally measured values [3]. A recent and more general description from the point of view of lubrication theory [7] seems to provide better predictions. But this approach requires numerical computation and again at small flow rates the agreement with experiment decreases.

Here we are concerned with a surprising application of the circular hydraulic jump with respect to some of the most exotic objects thought to populate our universe: black holes. Indeed, the circular jump is assumed to constitute an effective white hole (the time-reverse of a black hole) for waves propagating at a speed c on the surface of the fluid ($c = \sqrt{gh}$ in the shallow-water gravity wave limit, with h the fluid height and g the gravitational constant). Theoretically, it is hypothesised (following

Rayleigh) that the flow decelerates across the jump from a supercritical flow in the inner region—where the radial fluid velocity at the surface v_r^s is such that $v_r^s > c$ so that surface ripples can only propagate downstream—to a subcritical flow outside, where $v_r^s < c$ and hence the ripples can propagate in both directions. Here, supercritical and subcritical typically refer to the value of the Froude number $Fr = v_r^s/\sqrt{gh}$ or the related Mach number $M = v_r^s/c$. In relativistic language, the jump would therefore constitute a one-directional membrane or white hole: surface waves outside the jump cannot penetrate in the inner region; they are trapped outside in precisely the same sense as light is trapped inside a black hole. This analogy can formally be written in relativistic language, as demonstrated by Unruh and Schützhold for long gravity waves effectively propagating in one dimension [8] and applied to the circular jump by Volovik [9, 10]. The essential point is similar to the case of acoustic black holes [11] and other examples of analogue gravity [12], namely that the propagation of these surface waves obeys a generalised d’Alembertian equation in which the intervening curved-spacetime metric is identical to the 2+1-dimensional Painlevé-Gullstrand form of the well-known Schwarzschild metric which describes black/white holes in relativity [13]. The role of the speed of light is played by the surface wave propagation speed c , while the radial surface flow velocity v_r^s corresponds to the local velocity of a freely falling observer in the Painlevé-Gullstrand metric. It is in this precise sense that the circular jump is believed to constitute the hydrodynamical analogue of a white hole or “gravitational fountain”.

However, a simple experimental proof that the circular jump indeed constitutes a white hole has so far not been provided. Two strategies could be pursued to provide such a proof. First, one could measure v_r^s and c separately and compare their values. Some measurements of the surface velocity exist, see [14] and references therein. But these are rather sparse for the inner region. This

is probably due to the high value of the speed of flow inside the jump and the complicated nature of its full profile (which could also have an important non-radial component). Moreover, the extreme thinness of the fluid film, typically thinner than a Particle Image Velocimetry laser sheet, means that such imagery methods should be handled with care. Even more complicated is the measure of the surface wave propagation velocity c . A direct measure could be performed by sending and tracking surface waves. Some complications that immediately come to mind are the dispersive nature of c , as well as the “backreaction” problem well-known in gravity, i.e., the influence of the wave itself on the geometry of the jump. Alternatively, one could measure the height h of the fluid and in principle derive c as $c = \sqrt{gh}$ plus possible dispersive corrections. But this induces an additional approximation which one would prefer to avoid. So from the point of view of the white hole analogy, direct measurements of v_r^s and c are probably not the best strategy. A second and better strategy is to measure the ratio v_r^s/c directly. Our demonstration follows this idea and relies on measurements of the Mach cone associated with the supercritical flow in the inner region of the jump.

It is well known that the envelope of the subsequent wavefronts emitted by an object moving at a supersonic speed forms an observable cone, the Mach cone [15]. The half-angle (or Mach angle) of the cone θ can be related to the speed of sound c_{so} and the propagation velocity v of the object through simple trigonometry: $\sin \theta = c_{so}/v = 1/M$ with M the Mach number. The same holds true for a point-like object at rest on the surface of a supercritical fluid flow ($v_r^s > c$) with c now the propagation speed of surface waves. Measurements of the Mach angle therefore allow to trace the ratio v_r^s/c in the supercritical region. θ should exactly equal $\pi/2$ at the hydrodynamic white hole horizon where $c = v_r^s$, and become complex (the Mach cone disappearing) in the subcritical region.

Experiments – Our experiment to demonstrate the presence of a hydrodynamic horizon consists of the following. Silicon oil was pumped through a steel nozzle and impacted on a square 30cm×30cm PVC plate placed inside the aquarium containing silicon oil. The impact plate rests on adjustable pillars calibrated horizontally using a spirit level. The silicon oil has the following nominal characteristics at room temperature: viscosity $\nu = 20\text{cS} \approx 20\nu_{\text{water}}$; surface tension $\gamma = 0.0206\text{N/m} \approx \frac{1}{3}\gamma_{\text{water}}$; density $\rho = 950\text{kg/m}^3$; capillary length $l_c = \sqrt{\gamma/g\rho} = 1.49\text{mm} \approx 0.5l_{c(\text{water})}$. The pump, a Pollard MPX06P, has a frequency range of 0-3150 rpm and is mounted with a stator head of 4cm³, leading to flow rates of $Q = 0 - 756\text{L/h}$. The flow rates were double-checked at low flow rates with a MacNaught MR100 (0-100L/h) digital flowmeter and found to be accurate within measurement error. The fluid height H far outside the jump can be imposed by adjusting the amount of oil in the aquarium. The height d of the nozzle

with respect to the impact plate can be varied. A LaVision HighSpeedStar 4G camera (1024×1024 pixels) is placed 1500mm above the aquarium. The images are calibrated using LaVision’s DaVis software and then exported into ImageJ for further analysis (e.g., to measure the Mach angle).

We have chosen silicon oil because it combines a rather high viscosity with a low surface tension. The high viscosity allows to maximise the laminarity of the flow, thereby avoiding turbulent effects which would complicate flow patterns. It also guarantees that we create type I circular jumps (with a smooth unidirectional surface flow) over a larger range of flow rates rather than type II jumps (which exhibit surface flow reversal currents near the jump radius) or even turbulent jumps like in water, see e.g. [3]. We indeed observed a transition at high flow rates between both types and the appearance of a rim and undulations characteristic for the type II jump, which would modify strongly the effective metric of the circular jump. A low surface tension moreover guarantees that we avoid polygonal or more complicated jump shapes [5]. Such effects might be interesting from a fluid mechanics’ point of view, but are detrimental to the gravitational analogy, which assumes circular symmetry and a smooth propagation of the surface waves. To our knowledge, the surface tension of our silicon oil is the lowest to be reported in any experiment on the circular jump, still 50% lower than the mineral oil used in [5]. This also implies that we can essentially neglect surface tension when calculating the jet radius, which then obeys the standard result $r_{\text{jet}}/a = (1 + 2/Fr_j^2)^{-1/4}$. Here, the Froude number for the jet is $Fr_j = \frac{Q/\pi a^2}{\sqrt{gz}}$, with a the nozzle radius and z the downward distance from the nozzle. The measured jet radius as a function of the flow rate agrees very well with the theoretical curve, as can be seen from Fig. 1 for $z = 13\text{mm}$. In particular, the jet radius saturates around $Fr_j \sim 2 - 3$. We have checked translation invariance by performing measures at different values of z (not reported). Fig. 1 also shows a typical example of the jump radius R_j versus flow rate Q as obtained in our experiments. The relation $R_j(Q)$ adapts well to a power law [16]. However, we have found that the best-fit exponent can vary substantially from one setup to another. Moreover, we have noticed a possible regime change in the $R_j(Q)$ -dependence. Above a certain threshold (perhaps related to but not necessarily equal to the saturation threshold of the jet), R_j seems to increase through a simple linear law with Q . We have verified that such a regime change is compatible with other data presented in the literature [17]. At even higher flow rates, imperfections such as a slight deviation from a perfectly vertical impact, imperfections in the interior of the nozzle, or the rugosity of the impact plate, break the circular symmetry of the jump. They also partially saturate the jump radius and finally desta-

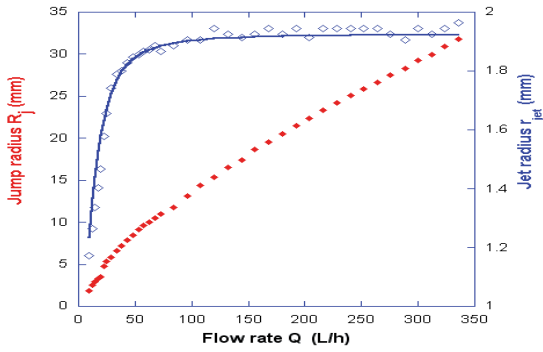


FIG. 1: Dependence of the jump radius R_j (red dots) and the fluid jet radius r_{jet} (blue line: theoretical curve, blue diamonds: experimental values measured at $z = 13\text{mm}$) on the flow rate Q . Experimental parameters: $d=76\text{mm}$, $a=1.925\text{mm}$, $H=0\text{mm}$.

bilise it completely. We will come back in future work to the apparent change of regime in the relation $R_j(Q)$ and explore its possible link with the saturation of the jet radius. Curiously, we have not found any reference where both data are presented together. For now, our main interest lies in the measurement of the Mach cone.

The Mach cones themselves are created as follows. A needle penetrates the flow surface at varying distance from the jet's impact point (the centre of the circular jump). Fig. 2 illustrates the process. Note that the cones' arms are not strictly straight, but slightly curved towards the exterior. We have therefore measured the Mach angle as close as possible to the needle. Our main result, the Mach angles θ as well as the resulting relation v_r^s/c , is presented in Fig. 3. The data of Fig. 3 correspond to a free circular jump ($H = 0\text{mm}$) created through a steel nozzle with radius $a = 4.75\text{mm}$ and a height $d = 62.5\text{mm}$, and at a flow rate of 240 L/h . We have chosen an intermediate flow rate in order to obtain a type I jump, and have also checked that the results do not depend qualitatively on H, a, d or Q , as long as one remains within a stable jump regime.

Inside the jet impact zone ($r < a$), we expect $v_r^s \ll c$ followed by a steep increase for $r \gtrsim a$ until a certain value $v_r^{s,\text{max}}$, since the fluid impacts vertically before being converted into a radial flow. The field of vision of our experimental setup starts near this maximum, see Fig. 3, corresponding to a Mach angle θ of roughly $\pi/10$. From there, θ smoothly increases to about $\pi/4$ at approximately $3/4$ of the jump radius, and then rapidly opens up to reach exactly $\pi/2$ near the ridge of the jump. This implies $v_r^s/c = 1$ and hence constitutes a clear proof that the jump indeed represents a white hole horizon for surface waves, independently of whether c is strictly equal to \sqrt{gh} or modified by dispersive corrections.

Saddle-node bifurcation – The fact that the circular jump represents a white hole horizon illustrates that the

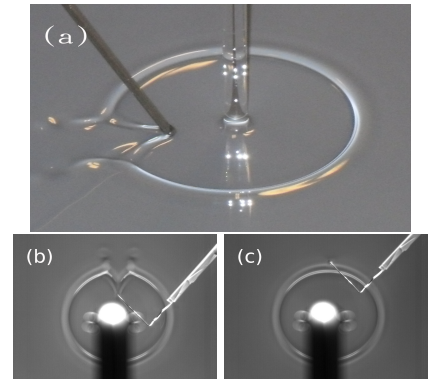


FIG. 2: (a) Mach cone in a circular hydraulic jump. (b) Mach cone measurement: A needle is placed inside the flow at varying distances from the centre of the jump. (c) The Mach cone disappears just outside of the jump. [The blurry object covering part of the cone in (b) and (c) is the nozzle holder.]

concept of horizons is not limited to relativity. This generality goes even further. Note that the Mach angles $\theta_W \in [0, \pi/2]$ and $\theta_B = \pi - \theta_W$ would lead to the same value of v_r^s/c , θ_W corresponding to a white hole (a source) and θ_B to a black hole (a drain). At the horizon itself, both solutions merge: $\theta_W = \theta_B = \pi/2$. This is an example of a saddle-node bifurcation in dynamical systems theory, as was earlier established in the deep-water gravity-wave regime [18]. Indeed, using an asymptotic development of $\arcsin(x)$ for $x \rightarrow 1$, one can write in the near-horizon region (for shallow-water waves and also e.g. for acoustic waves in a de Laval nozzle): $\theta = \arcsin(1 - \epsilon) \approx \pi/2(1 - \sqrt{\epsilon})$, where $\epsilon = 1 - c/v_r^s$. Inverting this relation, one obtains

$$\epsilon - \left(\frac{\pi/2 - \theta}{\pi/2} \right)^2 = 0.$$

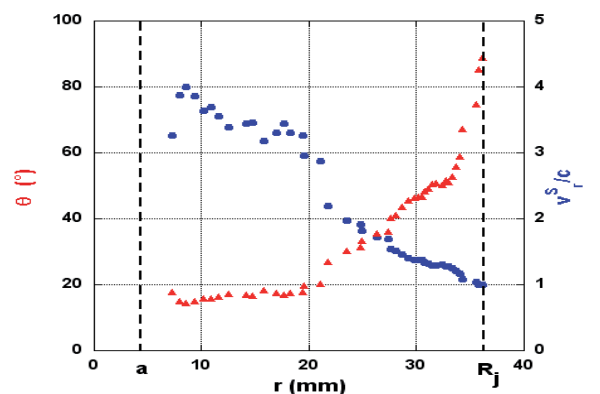


FIG. 3: Mach angle θ (red triangles) and ratio v_r^s/c (blue circles) as a function of the distance r from the centre of the jump. The dashed vertical lines represent the nozzle radius a and the jump radius R_j .

This is precisely the canonical expression of the stationary normal form for a spatial saddle-node bifurcation, with ϵ the control parameter and θ the order parameter [19]. It implies that the near-horizon behaviour inside a black/white hole is not only a common feature of typical analogue gravity systems involving sound or surface waves, but belongs to the universality class of saddle-node bifurcations in a dynamical-systems description.

Perspectives – The main current driving force behind analogue gravity is to study Hawking radiation, in stimulated form in classical systems [20–22] and ultimately in spontaneous form in quantum systems [23, 24]. The first point of interest is the laboratory reproducibility *in se* of the Hawking effect. Following the preliminary papers [20, 21], a first clear signal of a stimulated Hawking-type process in a hydrodynamic system was recently obtained in a wave-channel experiment [22]. The second point of interest is the robustness of Hawking radiation with respect to high-frequency “transplanckian” effects which could form a possible signal of quantum-gravitational corrections to relativity. We limit ourselves to a few remarks within this second context. The circular jump typically has a “superluminal” dispersion relation: the group velocity $c_g \equiv \frac{d\omega}{dk}$ increases with the wave number k . This can be checked by calculating c_g as a function of the fluid depth h from the dispersion relation $\omega^2 = (gk + \frac{\gamma}{\rho}k^3) \tanh(kh)$. Contrarily to the wave channel, this implies that the Hawking effect in the circular jump will inevitably involve processes occurring *inside* the horizon [25]. As a direct consequence, a “competition” is expected between the Hawking process and the so-called Miles instability. The latter consists in an amplification of high- k modes due to friction with a fixed boundary, and its onset is precisely when the fluid becomes supercritical. If there exists a transplanckian preferred frame in gravity, then friction with respect to this transplanckian “ether” could lead to a similar Miles instability. It has been suggested that this could affect the Hawking process by distorting the “thermal” balance between negative and positive frequency modes on opposite sides of the horizon [25], or that the Miles instability could actually become the dominant mechanism of dissipation of the black hole [9], reducing the Hawking radiation to a lower-order curiosity. We propose a third scenario. The Miles instability could simply create a threshold for the Hawking radiation. Such a scenario is well-known in fluid mechanics in the case of the Booker-Bretherton effect [26]. There, internal gravity waves can be either reflected at a turning point (corresponding to a group velocity horizon), or absorbed in a critical layer (corresponding to a phase velocity horizon). This absorption is subject to a threshold due to the Kelvin-Helmholtz instability. The resulting exponential attenuation factor for the energy is given by $\exp[-2\pi(Ri - 1/4)^{1/2}]$ in terms of the Richardson number $Ri = N^2/|U_z|^2$, with N the Brunt-Väisälä frequency, and U_z the vertical variation of

the horizontal velocity component at the critical layer. The derivation of this formula bares a striking resemblance to the derivation of Hawking radiation and, apart from being instructive with regard to the Hawking-Miles competition, could also shed an interesting light on the exact role of the phase and group velocities for horizon effects in the presence of dispersion.

-
- [1] L. Rayleigh, Proc. Roy. Soc. A **90**, 324 (1914).
 - [2] E. J. Watson, J. Fluid Mech. **20**, 481 (1964).
 - [3] J. W. M. Bush and J. M. Aristoff, J. Fluid. Mech. **489**, 229 (2003).
 - [4] C. Ellegaard, A. E. Hansen, A. Haaning, A. Marcussen, T. Bohr, J. Hansen, and S. Watanabe, Nature **392**, 767 (1998).
 - [5] J. W. M. Bush, J. M. Aristoff, and A. E. Hosoi, J. Fluid. Mech. **558**, 33 (2006).
 - [6] E. Dressaire, L. Courbin, J. Crest, and H. A. Stone, Phys. Rev. Lett. **102**, 194503 (2009).
 - [7] N. O. Rojas, M. Argentina, E. Cerda, and E. Tirapegui, Phys. Rev. Lett. **104**, 187801 (2010).
 - [8] R. Schützhold and W. G. Unruh, Phys. Rev. D **66**, 044019 (2002).
 - [9] G. E. Volovik, JETP Lett. **82**, 624 (2005).
 - [10] G. E. Volovik, J. Low Temp. Phys. **145**, 337 (2006).
 - [11] W. G. Unruh, Phys. Rev. Lett. **46**, 1351 (1981).
 - [12] C. Barceló, S. Liberati, and M. Visser, Living Rev. Rel. **8**, 12 (2005).
 - [13] A. K. Ray and J. K. Bhattacharjee, Phys. Lett. A **371**, 241 (2007).
 - [14] T. Bohr, V. Putkaradze, and S. Watanabe, Phys. Rev. Lett. **79**, 1038 (1997).
 - [15] L. D. Landau and E. M. Lifshitz, *Fluid Mechanics*, 2nd ed., Pergamon, UK (1987).
 - [16] T. Bohr, P. Dimon, and V. Putkaradze, J. Fluid Mech. **254**, 635 (1993).
 - [17] S. H. Hansen, S. Hørlyück, D. Zauner, P. Dimon, C. Ellegaard, and S. C. Creagh, Phys. Rev. E **55**, 7048 (1997).
 - [18] J.-C. Nardin, G. Rousseaux, and P. Couillet, Phys. Rev. Lett. **102**, 124504 (2009).
 - [19] M. Haragus and G. Iooss, *Local Bifurcations, Center Manifolds, and Normal Forms in Infinite-Dimensional Dynamical Systems*, EDP Sciences and Springer (2010).
 - [20] G. Rousseaux, C. Mathis, P. Maïssa, T. G. Philbin, and U. Leonhardt, New J. Phys. **10**, 053015 (2008).
 - [21] G. Rousseaux, P. Maïssa, C. Mathis, P. Couillet, T. G. Philbin, and U. Leonhardt, New J. Phys. **12**, 095018 (2010).
 - [22] S. Weinfurtner, E. W. Tedford, M. C. J. Penrice, W. G. Unruh, and G. A. Lawrence (2010), arXiv:1008.1911.
 - [23] I. Carusotto, S. Fagnocchi, A. Recati, R. Balbinot, and A. Fabbri, New J. Phys. **10**, 103001 (2008).
 - [24] F. Belgiorno, S. Cacciatori, M. Clerici, V. Gorini, G. Ortenzi, L. Rizzi, E. Rubino, V. Sala, and D. Faccio (2010), arXiv:1009.4634 (accepted by Phys. Rev. Lett.)
 - [25] W. G. Unruh and R. Schützhold, Phys. Rev. D **71**, 024028 (2005).
 - [26] J. R. Booker and F. P. Bretherton, J. Fluid Mech. **27**, 513 (1967).